A Universal Formulation for Multilevel Selective Harmonic Elimination - PWM with Half-Wave Symmetry

Angel Pérez-Basante, Salvador Ceballos, Georgios Konstantinou, *Senior Member, IEEE,* Josep Pou, *Fellow Member, IEEE,* Iñigo Kortabarria, and Iñigo Martínez de Alegría

Abstract—Selective harmonic elimination - pulse width modulation (SHE-PWM) can be utilized to improve the efficiency of multilevel voltage source converters due to its ability to provide low switching frequency and tight control of low-order harmonics. In addition, SHE-PWM with half-wave (HW) symmetry provides a higher number of solutions than quarter-wave (QW) symmetry and therefore, the waveform design can be improved. This work proposes a universal formulation, which can be utilized with HW symmetry, that provides a unique system of equations valid for any possible multilevel waveform. Thereby, without using predefined waveforms, this formulation provides the ability to search simultaneously both the firing angles and the switching patterns, simplifying significantly the search process and providing a high number of solutions. With the aim of selecting the optimum sets of firing angles, the solutions provided by HW and QW symmetries are compared, based on several metrics of harmonic performance, for particular test cases. Experimental results also validate the universal formulation with HW symmetry.

Index Terms—Selective harmonic elimination (SHE), multilevel voltage source converter (MVSC), quarter-wave (QW) symmetry, half-wave (HW) symmetry, universal formulation.

I. INTRODUCTION

Medium voltage (MV) converters have acquired high relevance for high power industrial and traction applications [2], [3], as well as renewable energy sources [4]. In particular, the number of installations of multilevel voltage source converters (MVSCs) in MV applications have increased considerably during last years [5]. MVSCs provide several advantages with respect to 2-level converters such as lower effective switching frequency, higher efficiency, lower dV/dt, smaller and simpler harmonic filters, lower common-mode voltage and lower insulation requirements [5].

Selective harmonic elimination - pulse width modulation (SHE-PWM) is a low switching frequency modulation technique which provides simultaneously tight control of low-order harmonics and low switching losses [6]. In this sense, the employment of this modulation in MVSCs when the number of levels is not high, as those used in medium voltage applications, is interesting [2], [7].

Most of the publications in the technical literature which solve the SHE-PWM problem employ predefined switching patterns to search the firing angles [6], [8]–[20]. However, in the case of multilevel converters where the number of possible waveforms is high, a particular predefined waveform could not be useful to find a solution for a particular modulation index, m_a, value. If there is no solution, a new predefined waveform should be utilized. In addition, different switching patterns are required to find a solution throughout the m_a range.

This issue has been addressed by [21], [22] utilizing a universal formulation which is valid for any possible waveform with QW symmetry. In this way, without using predefined waveforms, the search algorithm provides simultaneously the switching patterns and the associated firing angles, simplifying significantly the search process. In addition, due to the utilization of optimization algorithms, this technique is able to calculate a high number of firing angles. On the other hand, a unified formulation with QW symmetry has also been presented by [23]. This unified formulation, where predefined waveforms are not required, is applied along with the theory of Groebner bases to obtain the solutions. However, due to the high computational load of Groebner bases theory, the maximum number of firing angles which can be solved utilizing standard personal workstations is 9 [24].

Most of technical publications dealing with SHE-PWM for MVSCs focus on the QW symmetry. However, the HW symmetry provides a higher number of solutions than QW and different phase values for every harmonic [25]. Therefore, the design of the SHE-PWM waveform can be further optimized with HW symmetry [9], [26]. This work provides a universal formulation which can be applied with HW symmetry. The system of equations provided by this formulation has been solved utilizing genetic algorithms (GAs) due to their proven effectiveness [7], [8], [15], [22], [25], [27]–[37]. The main contributions of the paper are:

A. Pérez-Basante and S. Ceballos are with the Energy and Environment Division, Tecnalia Research and Innovation, 48160 Derio, Spain (e-mail: angel.perez@tecnalia.com; salvador.ceballos@tecnalia.com)

I. Kortabarria and I. Martínez de Alegría are with the Electronic Technology Department, University of the Basque Country (UPV/EHU), 48013 Bilbao, Spain (e-mail: inigo.kortabarria@ehu.eus; inigo.martinezdealegria@ehu.eus).

J. Pou is with the School of Electrical and Electronic Engineering, Nanyang Technological University, 639798 Singapore (e-mail: j.pou@ntu.edu.sg)

G. Konstantinou is with the School of Electrical Engineering and Telecommunications, University of New South Wales, Sydney, NSW 2052, Australia (e-mail: g.konstantinou@unsw.edu.au)

Fig. 1. Phase-neutral voltage, v_{a0}. Switching scheme of SHE-PWM with HW symmetry.

Fig. 2. Process to solve the SHE-PWM problem for a particular m_a with the traditional formulation.

- A new universal formulation of the SHE-PWM problem with HW symmetry is presented. Unlike conventional formulations, it has the ability to find solutions without using predefined voltage waveforms. Consequently, only one set of equations is used to solve the SHE-PWM problem and therefore, the search algorithm is able to provide simultaneously the switching patterns and the associated firing angles. In this way, the searching process is significantly simplified.
- Different solutions, utilizing the existing universal formulation with QW symmetry [22] and the proposed universal formulation with HW symmetry, are obtained throughout the m_a range. Among all the solutions obtained, the optimum solutions are selected with regard to several metrics. A study has been realized which provides deep insights into the different solutions and drives several conclusions.

The rest of this paper is organized as follows. Section II describes the commonly used formulation to implement SHE-PWM with HW symmetry, while Section III describes the novel universal formulation proposed in this paper. A comparison between the proposed and traditional formulations is presented in Section IV. Section V provides a deep analysis of the solutions obtained, throughout the m_a range, for test cases with HW and QW solutions, based on particular metrics. The experimental results are described in Section VI. Finally, Section VII concludes the paper.

II. CURRENT FORMULATION TO SOLVE SHE-PWM WITH HALF-WAVE (HW) SYMMETRY: PREDEFINED SWITCHING PATTERNS

The scheme of a SHE-PWM waveform with HW symmetry is depicted at Fig. 1, whose Fourier series expansion is given by (1), where a_n and b_n are the Fourier series coefficients and ω is the fundamental frequency [6], [9], [26]. This waveform, in case of three phase systems, may contain odd non-triplen harmonics besides the fundamental one.

$$v_{a0} = \sum_{n=1}^{\infty} a_n cos(n\omega t) + \sum_{n=1}^{\infty} b_n sin(n\omega t), \qquad (1)$$

With the aim of solving the SHE-PWM problem, the firing angles located in the first half fundamental cycle must be calculated to control the lower-order harmonics. SHE-PWM with HW symmetry re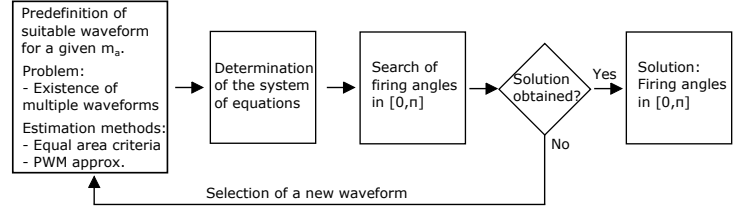quires twice as many different firing angles than SHE-PWM with QW symmetry [6] because unlike QW symmetry, both a_n and b_n must be controlled. Therefore, $2l$ angles must be calculated to eliminate l harmonics. In this way, the number of controlled harmonics are equal for both symmetries, although HW symmetry could provide non-eliminated harmonics with different phase values, obtaining a wider variety of solutions.

The equations of a_n and b_n are given by (2) and (3) [26], respectively, according to the rising and falling edges depicted at Fig. 1, where L is the number of levels, V_L is the step voltage, θ_k are the firing angles and p_k is given by (4). Therefore, there is a different equation system, with distinct p_k values, for every switching pattern.

$$a_n = -\frac{2V_L}{n\pi} \sum_{k=1}^{2l} p_k sin(n\theta_k), \qquad (2)$$

$$b_n = \frac{2V_L}{n\pi} \sum_{k=1}^{2l} p_k cos(n\theta_k), \qquad (3)$$

$$p_k = \left\{ \begin{array}{l} 1 \ \forall \ rising \ edge, \\ -1 \ \forall \ falling \ edge, \end{array} \right\}, \qquad (4)$$

$$0 \leq \theta_1 < \theta_2 < ... < \theta_{2l} \leq \pi, \qquad (5)$$

With the aim of solving (2) and (3), previously published methods (for instance [6], [9], [26]) predefine the switching pattern defining the sign of every step, p_k, and the order of the firing angles, as it is given by (5), before starting the search of the firing angles throughout the m_a range (see Fig. 2). This fact hinders the searching task significantly in case of MVSCs because the number of possible predefined switching patterns is very high and increases as the number of levels increases. Many of these patterns do not provide any useful solution for a particular m_a value. In this way, several techniques have been used to estimate which possible waveform could be useful to solve the SHE-PWM problem for that m_a. In particular, the waveform provided by multicarrier PWM or by the method of equal area with superposition of center of gravity [26], [38] could be used. However, the search of solutions depends on the effectiveness of these estimation methods. As it is shown in Fig. 2, if the predefined waveform does not provide a solution, a new waveform must be utilized. Therefore, avoiding the requirement of predefining the waveform is desirable.

III. PROPOSED UNIVERSAL FORMULATION FOR SHE-PWM WITH HALF-WAVE SYMMETRY

The proposed universal formulation provides a unique system of equations which is valid for every possible waveform. In this way, it is possible to search simultaneously the firing angles and the switching patterns which solve the SHE-PWM problem, without utilizing predefined waveforms, simplifying significantly the searching task. As stated before, this feature is important in MVSCs where there are many different possible waveforms and many of them could not be valid to find a solution for a particular m_a. The proposed system of equations can be solved with different existing search methods, such as optimization algorithms (offline technique) [6] or generalized hopfield neural networks (online technique) [39]. GAs have been selected to solve the proposed system of equations (the search algorithm is described in detail in [22]) due to their ability to find a high number of firing angles. In addition, the firing angles calculated offline, which are stored in look-up tables, could be utilized along with techniques such as model predictive control (MPC), in such a way that the transient behaviour of converters can be improved [3].

A. System of Equations

The proposed universal formulation modifies the equations of a_n and b_n given by (2) and (3), respectively. The new equations are given by (6), (7) and (8). As it can be noticed:

- Equations (6) and (7) do not depend on the switching pattern (variables p_k are not utilized). There are no positive signs in (6) nor negative signs in (7), which represent the negative steps. In order to provide waveforms with positive and negative steps, the concept of virtual firing angles, $\theta_{k,v}$, is introduced. These virtual firing angles are searched in the range $[0, 2\pi]$ unlike conventional firing angles which are searched in $[0, \pi]$ [26]. In this way, the virtual angles will provide simultaneously information about the switching pattern and the real firing angles (see Section III-B).

- In addition, there is not constraint in the order of firing angles, unlike it is done in previous works [6], [9], [26].

$$a_n = -\frac{2V_L}{n\pi} \sum_{k=1}^{2l} sin(n\theta_{k,v}), \qquad (6)$$

$$b_n = \frac{2V_L}{n\pi} \sum_{k=1}^{2l} cos(n\theta_{k,v}), \qquad (7)$$

$$0 \leq \theta_{k,v} \leq 2\pi, \qquad (8)$$

As a result, a unique system of equations, which is valid for any possible waveform, is provided to solve the SHE-PWM problem with HW symmetry. The proposed system of equations is given by (9) and (10) for a_n and b_n coefficients, respectively, where $2l$ is the number of firing angles that will be calculated in the first HW, $\theta_{k,v}$ is the identifier of every virtual firing angle, n is the identifier of every harmonic and L is the number of levels. The triplen harmonics are not regarded because a three-phase MVSC is considered. A_1 and

B_1 values must comply with (11) and (12), where ϕ_1 is the phase of the fundamental harmonic and m_a is the modulation index. Finally, ε_{an} and ε_{bn} represent the errors provided by the search algorithm for the a_n and b_n coefficients, respectively. The search algorithm will try to minimize these errors.

$$\frac{2}{\pi(L-1)}(-\sin(\theta_{1,v}) - \sin(\theta_{2,v}) - ... $$
$$... - \sin(\theta_{2l,v})) - A_1 = \varepsilon_{a1},$$
$$\frac{2}{5\pi(L-1)}(-\sin(5\theta_{1,v}) - \sin(5\theta_{2,v}) - ...$$
$$... - \sin(5\theta_{2l,v})) = \varepsilon_{a5}, \qquad (9)$$
$$\vdots$$
$$\frac{2}{n\pi(L-1)}(-\sin(n\theta_{1,v}) - \sin(n\theta_{2,v}) - ...$$
$$... - \sin(n\theta_{2l,v})) = \varepsilon_{an},$$

$$\frac{2}{\pi(L-1)}(\cos(\theta_{1,v}) + \cos(\theta_{2,v}) + ...$$
$$... + \cos(\theta_{2l,v})) - B_1 = \varepsilon_{b1},$$
$$\frac{2}{5\pi(L-1)}(\cos(5\theta_{1,v}) + \cos(5\theta_{2,v}) + ...$$
$$... + \cos(5\theta_{2l,v})) = \varepsilon_{b5}, \qquad (10)$$
$$\vdots$$
$$\frac{2}{n\pi(L-1)}(\cos(n\theta_{1,v}) + \cos(n\theta_{2,v}) + ...$$
$$... + \cos(n\theta_{2l,v})) = \varepsilon_{bn},$$

$$\sqrt{A_1^2 + B_1^2} = \frac{m_a}{2}, \quad 0 < m_a < \frac{4}{\pi}, \qquad (11)$$

$$\phi_1 = arctg\left(\frac{B_1}{A_1}\right), \qquad (12)$$

B. Translation from Virtual into Real Firing Angles: Resulting Waveform

Once the solution (the set of virtual firing angles which are searched in $[0,2\pi]$) has been obtained, the virtual firing angles must be translated into real firing angles, θ_k, and the resulting waveform must be provided. The proposed translation is the following one (see Fig. 3):

- Virtual firing angles $\theta_{k,v}$ located in $[0,\pi]$ represent positive steps in the first HW and their actual value is given by (13).

$$\theta_k = \theta_{k,v}, \qquad (13)$$

- Virtual firing angles $\theta_{k,v}$ located in $[\pi, 2\pi]$ represent negative steps in the first HW and their actual value is given by (14). This fact is justified by (15) and (16).

$$\theta_k = \theta_{k,v} - \pi, \qquad (14)$$
$$cos(n\theta_{k,v}) = cos(n(\theta_k + \pi)) = cos(n\theta_k)cos(n\pi) =$$
$$= -cos(n\theta_k) \ \forall n \ odd, \qquad (15)$$
$$sin(n\theta_{k,v}) = sin(n(\theta_k + \pi)) = sin(n\theta_k)cos(n\pi) =$$
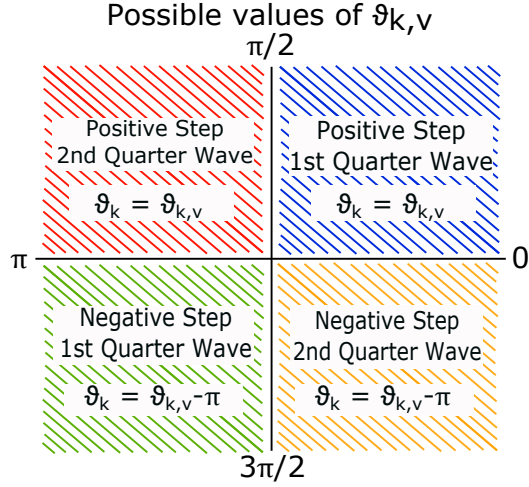$$= -sin(n\theta_k) \ \forall n \ odd, \qquad (16)$$

Fig. 3. Possible values of $\theta_{k,v}$ and its corresponding real angle value θ_k. Depending on the quarter-wave, between 0 and 2π radians, $\theta_{k,v}$ can represent positive or negative steps in the 1st or 2nd quarter wave.
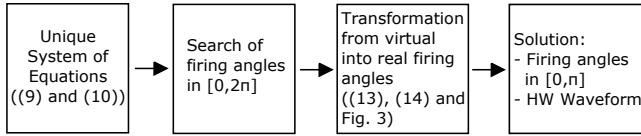

Fig. 4. Process to solve the SHE-PWM problem for a particular m_a with the proposed universal formulation.

Therefore, predefined waveforms are not required to obtain the solutions, as it is shown in the flow diagram of Fig. 4. Comparing with previous methods [6], [9], [26], the search of firing angles is significantly simplified and a high number of different waveforms with HW symmetry can be found.

C. Objective Function

To solve the set of equations given by (9)-(12), the search algorithm described in [22], which is based on genetic algorithms, is used. It makes use of an objective function which needs to be minimized to find an adequate set of firing angles. The objective function, F, utilized in this work is given by (17), where ε_{an} and ε_{bn}, given by (9) and (10), are the errors provided by the algorithm for the a_n and b_n coefficients, respectively, being n the identifier of every harmonic. On the other hand, f_{valid} is a function which checks the validity of the obtained waveform, considering the number of levels of the converter and the initial level, $L_{initial}$ and final level, L_{final}, of the half wave. Due to the HW symmetry, these levels must be equal but with opposite signs, as it is shown at Fig. 5 and they will be input parameters for the genetic algorithm.

$$F = \varepsilon_{a1}^2 + \varepsilon_{b1}^2 + \varepsilon_{a5}^2 + \varepsilon_{b5}^2 + ... + \varepsilon_{an}^2 + \varepsilon_{bn}^2 + \\ + f_{valid}(\theta_{1,v}, \theta_{2,v}, ..., \theta_{2l,v}), \quad (17)$$

The procedure to calculate f_{valid} consists of the following steps:
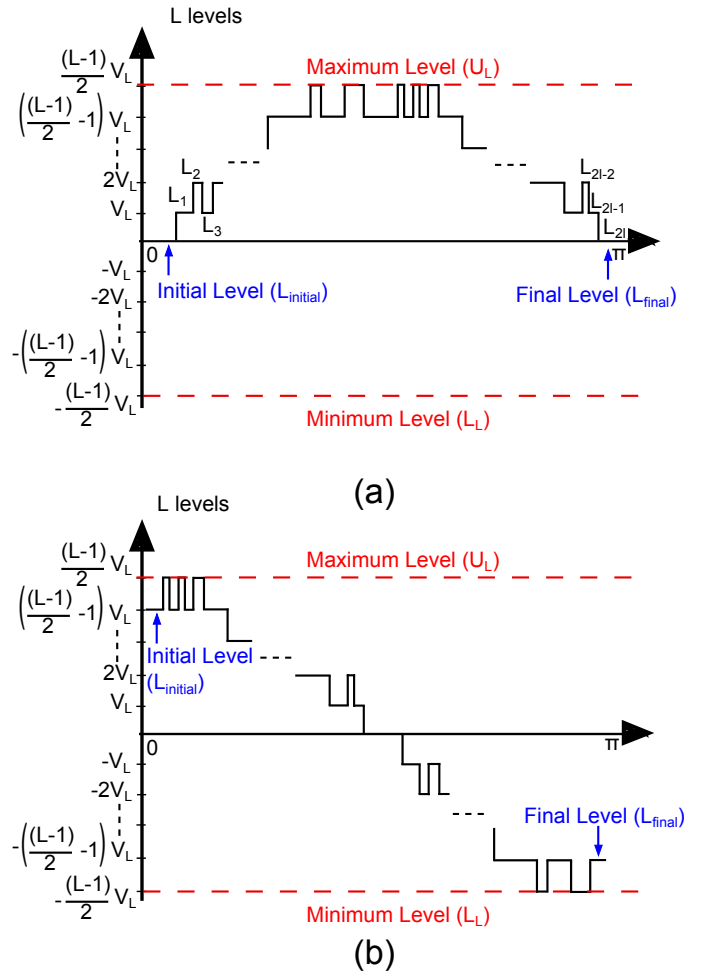
Fig. 5. Validity restrictions. (a) Half-wave with initial value 0. (b) Half-wave with initial value $(((L-1)/2)-1)V_L$.

- Calculation of $\theta_1, \theta_2, ..., \theta_{2l}$, from $\theta_{1,v}, \theta_{2,v}, ..., \theta_{2l,v}$, and the sign of their corresponding steps, as it is detailed in Section III-B.
- Calculation of the order, from lower to higher value, of $\theta_1, \theta_2, ..., \theta_{2l}$.
- Once the order of $\theta_1, \theta_2, ..., \theta_{2l}$ has been calculated, the level, L_i, of the waveform after every consecutive, j, firing angle is given by (18a) and (18b), as it is shown at Fig. 5-(a).

$$L_i = L_{initial} + \sum_{j=1}^{i} p_j, \quad 1 \le i \le 2l, \quad (18a)$$

$$p_j = \left\{ \begin{array}{l} 1 \ \forall \ rising \ edge, \\ -1 \ \forall \ falling \ edge, \end{array} \right\} \quad (18b)$$

- Finally, f_{valid} is given by (19) and (20), where U_L and L_L are the maximum and minimum achievable levels of the voltage waveform and $L_{initial}$ is the initial level of the waveform. If any level of the voltage waveform, L_i, is higher than U_L or lower than L_L or the final level, L_{final}, of the waveform after half a period is different to the opposite of the initial level, the solution provided by

the genetic algorithm is not valid. Consequently, f_{valid} returns a high value, H, that makes the objective function, F, take a high value (higher than the convergence threshold value) and the genetic algorithm reject the solution. Otherwise, if the solution is valid, f_{valid} would return 0. Valid HW symmetry waveforms are those which provide voltage levels that fall between the maximum and minimum allowed levels, besides $L_{final} = -L_{initial}$ (see Fig. 5). In this way, F would only provide the errors in the amplitude of every a_n and b_n coefficients and therefore, the optimization algorithm will be able to optimize that error and to find a solution.

$$f_{valid} = \begin{cases} H, \ if \ \left\{ \begin{array}{c} \exists L_i > U_L \ or \ \exists L_i < L_L \ or \\ L_{final} \neq -L_{initial} \end{array} \right\}, 1 \leq i \leq 2l \\ 0, \ if \ \left\{ \begin{array}{c} L_i \leq U_L \ \& \ L_i \geq L_L \ \& \\ L_{final} = -L_{initial} \end{array} \right\}, 1 \leq i \leq 2l \end{cases}, \tag{19}$$

$$H > Convergence \ Threshold \ Value, \tag{20}$$

In this way, utilizing the proposed objective function, the algorithm will always provide valid solutions.

D. Symmetric Solutions

It is worth noting that for every HW solution, when the fundamental phase $\phi_1 = \pi/2$, there is another symmetric solution with identical harmonic content, whose angle values for positive and negative steps, $\theta_{k,ps-sym}$ and $\theta_{k,ns-sym}$, are given by (21) and (22), respectively, where $\theta_{k,ps}$ and $\theta_{k,ns}$ are the positive and negative firing angles in the original HW solution and $2l$ is the total number of firing angles in the first half wave [25].

An example of these waveforms is depicted at Fig. 6, where different solutions for $m_a = 0.3$ and $L_{initial} = 0$, $L_{initial} = 1$ and $L_{initial} = -1$ are shown. Figs. 6-(a) and 6-(b) show symmetric solutions when $L_{initial} = 0$, whose firing angles are related by (21) and (22). Both waveforms have identical harmonic content but belong to different continuous sets of firing angles because of the different waveforms. In this way, for every obtained solution, two different sets of firing angles can be provided.

In a similar way, Figs. 6-(c) and 6-(d) show symmetric solutions when $L_{initial} = 1$ and $L_{initial} = -1$. Consequently, due to this symmetry only positive values of $L_{initial}$ can be considered to find the sets of firing angles, thus simplifying the searching process.

$$\theta_{k,ps-sym} = \pi - \theta_{(2l+1)-k,ns}, \tag{21}$$
$$\theta_{k,ns-sym} = \pi - \theta_{(2l+1)-k,ps}, \tag{22}$$

IV. COMPARISON OF PROPOSED AND CURRENT FORMULATIONS

With the aim of comparing the search processes when the traditional and universal formulations are applied, an empirical example of both processes is included. In addition, another example is presented to describe deeply the operation of the
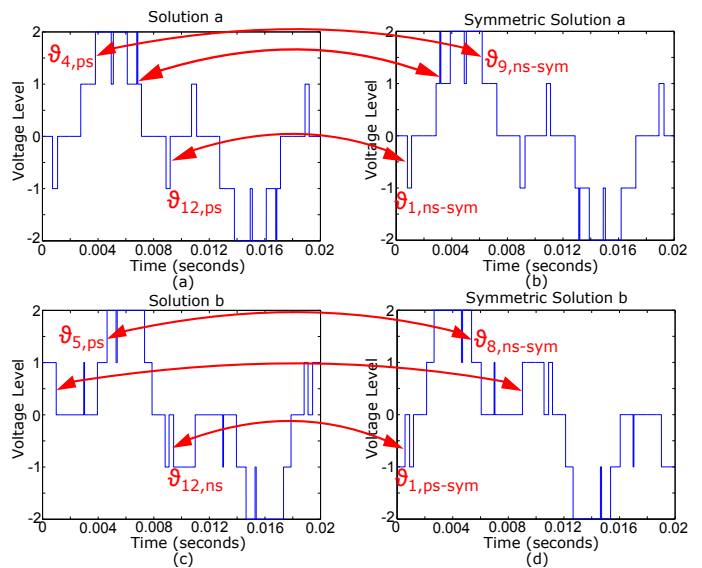

Fig. 6. MVSC with 9 levels and 12 firing angles in the first HW. (a) HW solution with $L_{initial} = 0$ and $m_a = 0.3$. (b) Symmetric HW solution with $L_{initial} = 0$ and $m_a = 0.3$. (c) HW solution with $L_{initial} = 1$ and $m_a = 0.3$. (d) Symmetric HW solution with $L_{initial} = -1$ and $m_a = 0.3$.

proposed universal formulation. In both examples, solutions for a converter with 9 levels, $m_a = 0.5$ and 12 firing angles in the first HW, are searched. Therefore, the harmonics eliminated are 5th, 7th, 11th, 13th and 17th. Finally, the advantages of the proposed universal formulation with respect to the traditional formulation are highlighted.

A. Examples of Application of Proposed and Traditional Formulations

Fig. 7 shows the application of traditional and proposed formulations to solve the SHE-PWM problem with HW symmetry for the converter commented previously. In both cases, the same solution has been found. Thereby, the differences between the search processes when the traditional and proposed formulations are applied can be noticed. In the traditional process, the waveform has been predefined beforehand to start the search of firing angles. Otherwise, in the proposed search process, it is not required to consider the waveform because it is given as part of the solution due to the employment of virtual firing angles.

In addition, Fig. 8 presents an empirical example where the proposed unique system of equations is utilized. As it can be noticed, with only one system of equations, utilizing virtual firing angles (which are searched in $[0,2\pi]$), it is possible to find solutions with different waveforms. In this way, as it has been commented previously, the search method that utilizes the proposed formulation will provide not only the firing angles but also the waveforms.

B. Main Advantages of the Proposed Universal Formulation

The method proposed in this paper to implement the SHE-PWM waveform with HW symmetry presents the following main features:

Traditional Method

Predefinition of Waveform

Application of
Estimation Method
for ma=0.5
$\phi_1 = \pi/2$

$\vartheta_1, \vartheta_2, \vartheta_3, \vartheta_4, \vartheta_5, \vartheta_6, \vartheta_7, \vartheta_8, \vartheta_9, \vartheta_{10}, \vartheta_{11}, \vartheta_{12}$

0   π

Formulation of System of Equations → (2), (3), (4) and (5)

Traditional System of Equations
Generalized for n^{th} harmonic

A_n Coefficients

$-\sin(n\vartheta_1)-\sin(n(\vartheta_2))+\sin(n\vartheta_3)+...$
$-\sin(n\vartheta_4)-\sin(n\vartheta_5))+\sin(n\vartheta_6)+...$
$+\sin(n\vartheta_7))-\sin(n\vartheta_8))+\sin(n\vartheta_9)+...$
$-\sin(n\vartheta_{10})+\sin(n\vartheta_{11})+\sin(n\vartheta_{12}))$

B_n Coefficients

$\cos(n\vartheta_1)+\cos(n(\vartheta_2))-\cos(n\vartheta_3)+...$
$+\cos(n\vartheta_4)+\cos(n\vartheta_5))-\cos(n\vartheta_6)+...$
$-\cos(n\vartheta_7))+\cos(n\vartheta_8))-\cos(n\vartheta_9)+...$
$+\cos(n\vartheta_{10})-\cos(n\vartheta_{11}))-\cos(n\vartheta_{12}))$

$\vartheta_1<\vartheta_2<\vartheta_3<\vartheta_4...<\vartheta_{12}$

Search of firing angles in [0, π] with GAs

Solution

ϑ_1=0.2504	ϑ_7=2.1554
ϑ_2=0.9751	ϑ_8=2.3262
ϑ_3=1.3907	ϑ_9=2.548
ϑ_4=1.4369	ϑ_{10}=2.6955
ϑ_5=1.7713	ϑ_{11}=2.7312
ϑ_6=1.8553	ϑ_{12}=2.7323

radians

Resulting Solution

Proposed Method

Unique System of Equations
Generalized for n^{th} harmonic

A_n Coefficients

$-\sin(n\vartheta_{1,v})-\sin(n\vartheta_{2,v})-\sin(n\vartheta_{3,v})-...$
$-\sin(n\vartheta_{4,v})-\sin(n\vartheta_{5,v})-\sin(n\vartheta_{6,v})-...$
$-\sin(n\vartheta_{7,v})-\sin(n\vartheta_{8,v})-\sin(n\vartheta_{9,v})-...$
$-\sin(n\vartheta_{10,v})-\sin(n\vartheta_{11,v})-\sin(n\vartheta_{12,v})$

B_n Coefficients

$\cos(n\vartheta_{1,v})+\cos(n\vartheta_{2,v})+\cos(n\vartheta_{3,v})+...$
$+\cos(n\vartheta_{4,v})+\cos(n\vartheta_{5,v})+\cos(n\vartheta_{6,v})+...$
$+\cos(n\vartheta_{7,v})+\cos(n\vartheta_{8,v})+\cos(n\vartheta_{9,v})+...$
$+\cos(n\vartheta_{10,v})+\cos(n\vartheta_{11,v})+\cos(n\vartheta_{12,v})$

Search of virtual firing angles in [0, 2π] with GAs

Virtual Solution

$\vartheta_{1,v}$=1.7713	$\vartheta_{7,v}$=5.8739
$\vartheta_{2,v}$=5.5996	$\vartheta_{8,v}$=5.8728
$\vartheta_{3,v}$=0.2504	$\vartheta_{9,v}$=1.4369
$\vartheta_{4,v}$=0.9751	$\vartheta_{10,v}$=2.3262
$\vartheta_{5,v}$=4.5323	$\vartheta_{11,v}$=4.9969
$\vartheta_{6,v}$=2.6955	$\vartheta_{12,v}$=5.2970

radians

Translation into real firing angles applying (13) and (14)

Real Solution

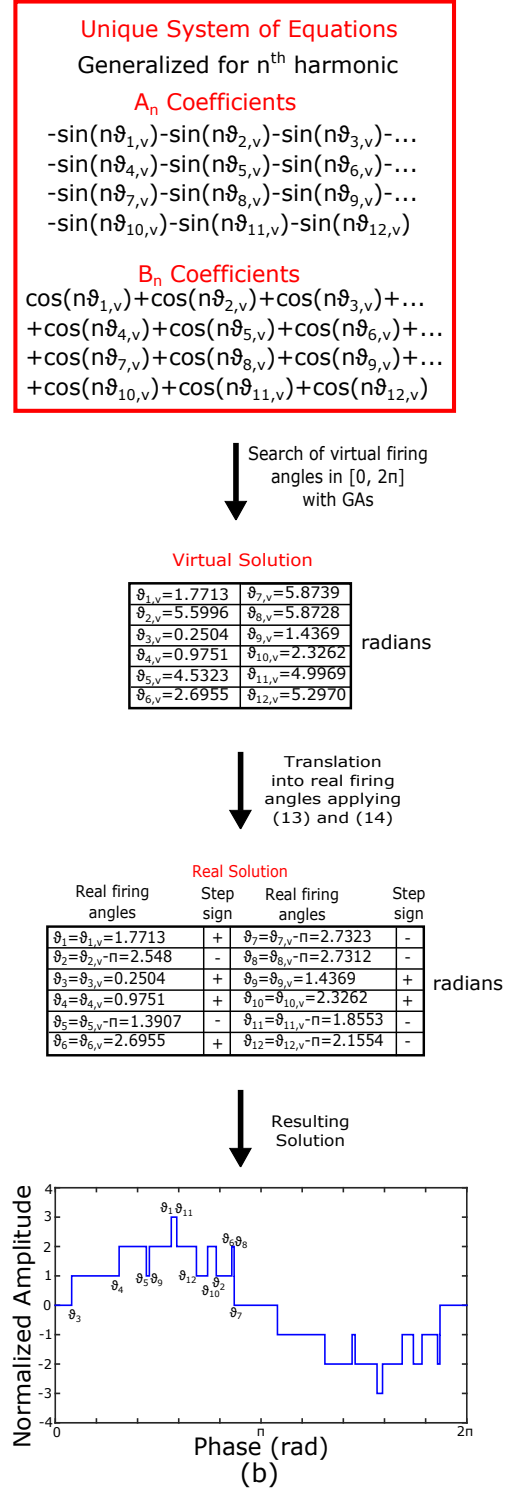| Real firing angles	Step sign	Real firing angles	Step sign
$\vartheta_1=\vartheta_{1,v}$=1.7713	+	$\vartheta_7=\vartheta_{7,v}$-π=2.7323	-
$\vartheta_2=\vartheta_{2,v}$-π=2.548	-	$\vartheta_8=\vartheta_{8,v}$-π=2.7312	-
$\vartheta_3=\vartheta_{3,v}$=0.2504	+	$\vartheta_9=\vartheta_{9,v}$=1.4369	+
$\vartheta_4=\vartheta_{4,v}$=0.9751	+	$\vartheta_{10}=\vartheta_{10,v}$=2.3262	+
$\vartheta_5=\vartheta_{5,v}$-π=1.3907	-	$\vartheta_{11}=\vartheta_{11,v}$-π=1.8553	-
$\vartheta_6=\vartheta_{6,v}$=2.6955	+	$\vartheta_{12}=\vartheta_{12,v}$-π=2.1554	-

radians

Resulting Solution

Fig. 7. Application of traditional and proposed formulation to obtain the same solution.

- The utilized system of equations is unique and valid for all possible waveforms, unlike previous works [6], [9], [26], [40]. This feature is provided by (13), (14), (15), (16) and the no constraint in the order of firing angles.
- Predefined waveforms are not required to obtain the solutions throughout the m_a and ϕ_1 ranges, unlike which is done in previous publications [26], [40]. Therefore, this technique is particularly interesting in case of multilevel voltage source converters, where the number of possible switching patterns is very high, simplifying significantly
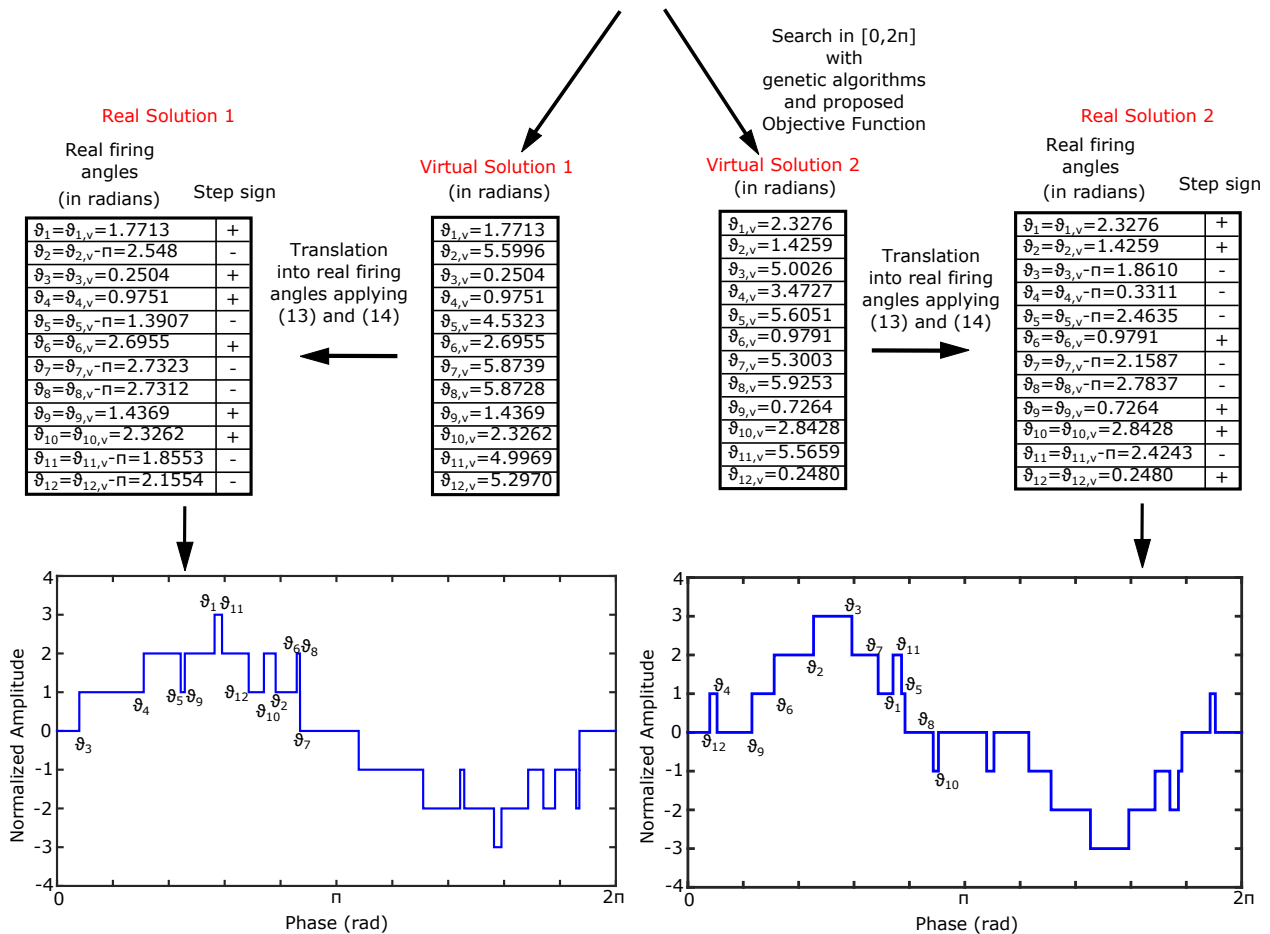
Fig. 8. Application of the proposed universal formulation for acquisition of multiple HW symmetrical solutions.

the search process.

- Due to the ability of providing any possible waveform, the proposed method is able to obtain a high number of different solutions for every m_a, as it is shown at Figs. 9 and 10 for $m_a = 0.3$ and $m_a = 1$, respectively.

- Longer continuous sets of firing angles can be obtained due to the lack of constraints in the order of firing angles and the no requirement of predefined waveforms. As it is shown in Figs. 11-Set1-(1), 11-Set3-(1) and 11-Set5-(1), there are crossings between firing angles whose step

sign is different, providing a change in the switching pattern. However, the continuous search does not stop at the crossing point because any possible waveform is considered by the method.

- An objective function, which always provides valid waveforms with HW symmetry, has been provided. This function can be utilized by optimization algorithms. In addition, this function provides the possibility of searching automatically the solutions with any possible initial level, $L_{initial}$, simplifying additionally the search.

V. ACQUISITION AND ANALYSIS OF SOLUTIONS WITH DIFFERENT SYMMETRIES

The universal formulation proposed in this work, along with the search algorithm described in [22], are able to find different solutions for every m_a value when HW symmetry is considered. This is possible because for every m_a value, different random initial populations are utilized at every algorithm execution. In addition, QW solutions can also be found if the universal formulation proposed by [22] is utilized. Therefore, multiple solutions with different symmetries can be found for every m_a, each one with its own characteristics, providing the possibility of optimizing different performance factors.

A. Case Studies

With the aim of performing a comparison between HW and QW solutions and drive several conclusions, 2 different case studies have been considered:

- Case I-QW: MVSC with 9 levels and 6 firing angles with QW symmetry.
- Case II-HW: MVSC with 9 levels and 12 firing angles with HW symmetry and $\phi_1 = \pi/2$.

Table I shows the total number of discrete solutions obtained for every m_a value and case study. To obtain the QW solutions for every m_a, 20 executions of the search algorithm presented in [22] have been performed. In this way, several different solutions have been provided for every m_a. If the number of executions is increased, a higher number of different solutions can be obtained for every m_a.

In case of HW symmetry, for every m_a value, the search algorithm has been executed 20 times with every possible initial value, $L_{initial}$. Please note that for every solution with $L_{initial} = -x$, $0 =< x <= U_L$, there is a symmetric solution with $L_{initial} = x$ (see Section III-D). Therefore, all the HW solutions are grouped by values of $L_{initial} >= 0$. On the other hand, the utilized fundamental phase is $\phi_1 = \pi/2$, providing a sine wave. In this way, only solutions with $L_{initial} = 0$, $L_{initial} = 1$ and $L_{initial} = -1$ have been found. The solutions which provide an error in the objective function (17) lower than 10^{-6} were stored.

Table I highlights the ability of the proposed universal formulation together with GAs to find multiple solutions. For illustration purposes some of the solutions obtained for case study II-HW with $L_{initial} = 0$ and $L_{initial} = 1$ for $m_a = 0.3$ and $m_a = 1$ are depicted in Figs. 9 and 10, respectively.
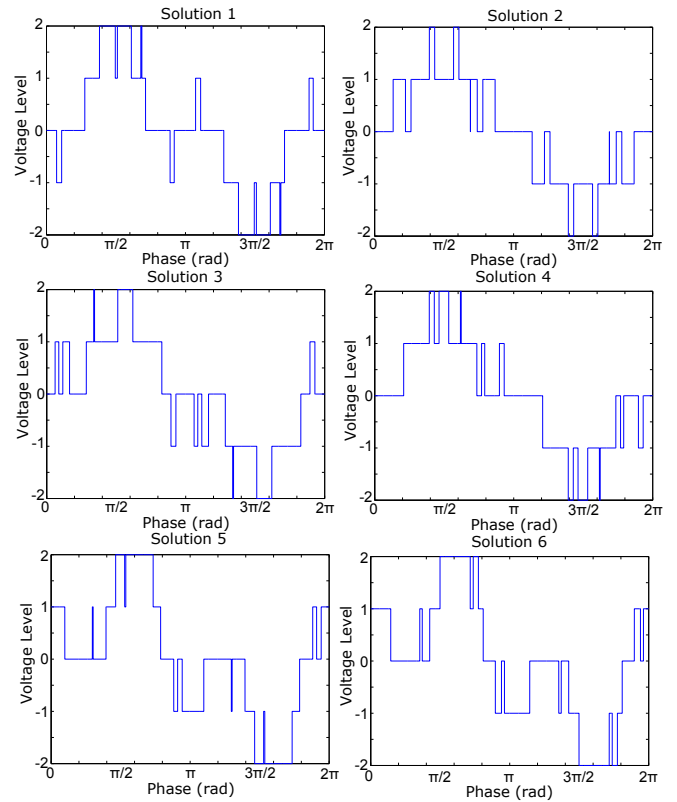

Fig. 9. Examples of HW solutions obtained for case II-HW with $m_a = 0.3$, $L_{initial} = 0$ and $L_{initial} = 1$ (amplitude normalized by V_L).

B. Performance Evaluation

To compare, classify and select the most suitable solution, several metrics of harmonic performance have been utilized [25]. In particular, this paper considers the following:

1) Total Harmonic Distortion (THD): The total harmonic distortion (THD) evaluates the total harmonic content of the waveform [9]. The triplen harmonics are not regarded due to the three-phase system.

2) Harmonic Distortion Factor (HDF): This factor provides the relevance of the first two non-eliminated harmonics. Regarding three-phase systems, the odd triplen harmonics will not be considered [25], [32].

3) Harmonic Loss Factor (HLF): This factor helps to estimate the losses. In particular, it is proportional to the weighted current total harmonic distortion (WTHD$_i$) [25].

4) Lower-Order Triplen Harmonics: Despite the fact that triplen harmonics are eliminated in three-phase systems, these harmonics increment the stress imposed on the insulation of grid transformers or motors [25]. Therefore, the analysis of triplen harmonic amplitudes should be considered. In particular, the third and ninth harmonics are regarded in this work.

C. Analysis of Solutions

Depending on the application, different performance criteria can be utilized to select the optimum solution. With the aim of reducing the converter losses, the solutions with the lowest HLF value for every m_a are selected in this paper. If several

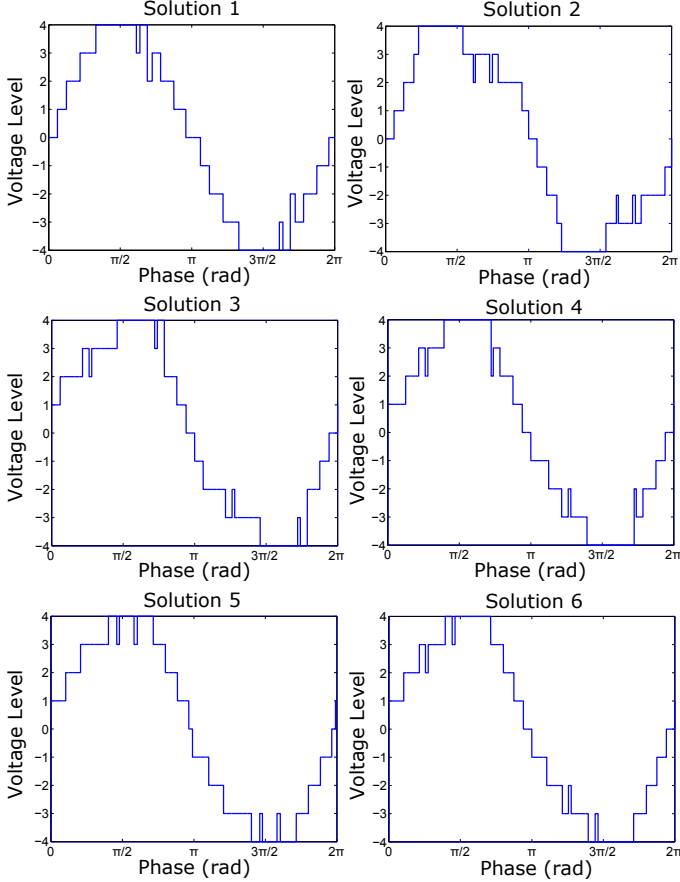| Case	Modulation Index											Total
	0.1	0.2	0.3	0.4	0.5	0.6	0.7	0.8	0.9	1	1.1	
Case I-QW	2	9	8	2	3	2	1	2	4	2	1	36
Case II-HW (Initial level 0)	9	10	9	4	7	10	10	3	7	2	4	75
Case II-HW (Initial level 1)	6	14	17	12	21	16	21	12	8	10	0	137

Fig. 10. Examples of HW solutions obtained for case II-HW with $m_a = 1$, $L_{initial} = 0$ and $L_{initial} = 1$ (amplitude normalized by V_L).

solutions provide the same HLF, the solution with the lowest third harmonic is selected. Table II shows the values of the performance factors for the selected solutions in cases I-QW and II-HW. In addition, the firing angles associated to the selected solutions of case II-HW are included in Appendix.

Regarding the case study II-HW, the continuous sets of firing angles, where solid and dashed lines represent positive and negative steps, respectively in the first HW, are included in Fig. 11. The sets have been calculated taking as initial point for the search algorithm those solutions included in Appendix. The performance factors associated with these firing angles have also been depicted in Fig. 11. This figure also shows how the THD and HLF reduce progressively, except for particular increments, when the m_a is increased. It is also shown at Fig. 11-Set 11-(2) how the over-modulation region provides an increment in the third harmonic.

As it can be noticed at Fig. 11, there are several gaps

in the m_a range where the search algorithm has not been able to find a proper solution which provides an error of the objective function lower than 10^{-6}. To fill these gaps, several intermediate solutions, different to those shown in Appendix, have been obtained and then utilized as starting points of the search algorithm. Using them, new continuous sets of firing angles, which are depicted at Fig. 12, have been acquired, completing the solutions throughout the m_a range. These sets of firing angles which determine the phase output voltage level are stored in look-up tables to control the multilevel converter. Depending on the type of multilevel converter, the switching states of its power devices are determined to obtain the desired phase output voltage level [7], [21], [22], [41].

Based on the results shown in tables I and II together with Figs. 11 and 12, the following conclusions can be derived:

- Unlike bipolar waveforms [25], in case of multilevel waveforms, the first two non-eliminated harmonics do not concentrate the majority of the harmonic energy. This fact can be noticed due to the big difference observed between the HDF and THD factors (see table II). Therefore, under the same THD value, the multilevel waveforms will provide lower HLF values than bipolar waveforms.

- Among all the solutions obtained for every m_a, at every case, the lowest value for every indicator may be provided by different solutions. In other words, for most of the m_a values at every case, there is no a single solution that provides the lowest value of all the defined metrics. Therefore, it will be required to determine a selection criteria depending on the application. As it has been commented, with the aim of improving the efficiency of the multilevel converter, the solutions with lowest HLF value have been selected in this work.

- Regarding the total number of solutions obtained throughout the m_a range, under equal number of levels and equal number of eliminated harmonics, HW solutions require twice as many firing angles to be calculated as QW solutions and therefore, the number of HW solutions obtained is higher, as it is shown in Table I [25]. In addition, the HW symmetry provides a higher number of solutions due to its ability to provide non-eliminated harmonics with different phase values [26]. Consequently, since more solutions are available with HW than with QW symmetry, HW symmetry has the potential capacity to find voltage waveforms with improved metrics. Nevertheless, there are particular cases where QW provides better solutions. In particular, the HLF (see Fig. 13) and THD (see Fig. 14) provided by both symmetries have been compared throughout the m_a range. As it can be noticed, depending on the m_a value, the best metric is provided

TABLE II
SOLUTIONS WITH LOWEST HLF FOR EVERY CASE: PERFORMANCE FACTORS (%)

| Case	Perf. Factor	Modulation Index										
		0.1	0.2	0.3	0.4	0.5	0.6	0.7	0.8	0.9	1	1.1
Case I-QW	THD (%)	90.76	40.84	24.20	21.78	15.02	13.63	12.92	9.19	7.17	8.61	7.52
	HDF (%)	67.11	18.94	5.60	12.52	9.80	4.48	5.99	4.04	1.74	2.54	1.66
	HLF (%)	3.43	1.20	0.68	0.76	0.53	0.39	0.39	0.29	0.17	0.26	0.23
	3rd Harm. (%)	44.07	42.80	24.75	54.20	16.01	16.95	41.85	12.24	14.66	3.23	8.23
	9th Harm. (%)	7.80	6.08	7.61	3.53	16.92	0.81	4.75	3.48	1.76	5.17	1.58
Case II-HW	THD (%)	94.27	40.84	24.69	21.08	15.64	11.02	10.42	9.66	7.47	8.15	7.40
	HDF (%)	38.24	13.35	7.46	9.53	8.98	3.64	3.86	3.10	1.33	3.64	3.66
	HLF (%)	3.38	1.22	0.72	0.69	0.50	0.29	0.29	0.29	0.17	0.24	0.24
	3rd Harm. (%)	255.00	186.12	37.46	62.83	51.90	54.02	18.54	17.68	11.82	18.09	9.52
	9th Harm. (%)	44.97	17.17	36.77	23.60	18.69	12.83	12.26	8.24	10.86	6.89	2.59
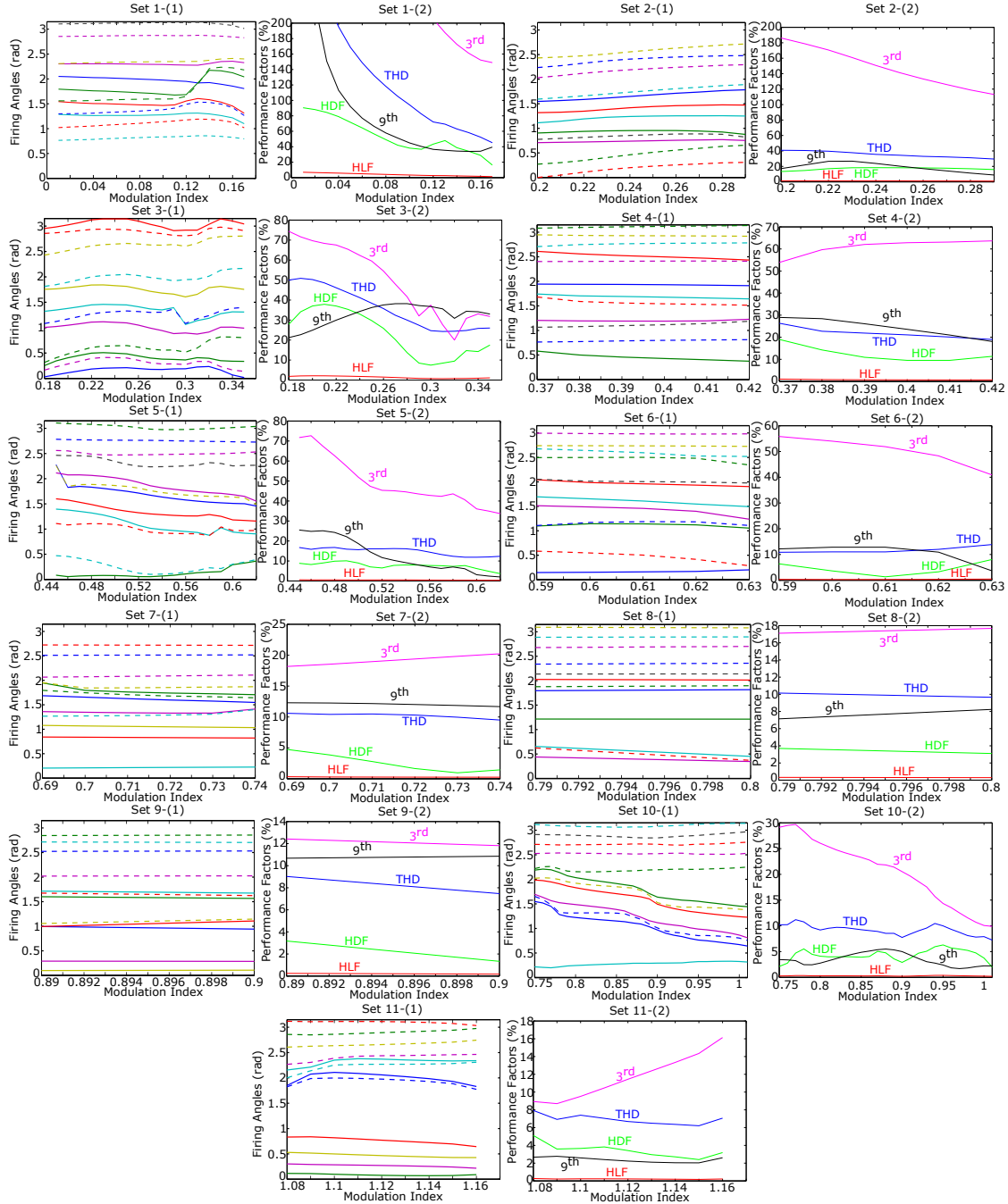
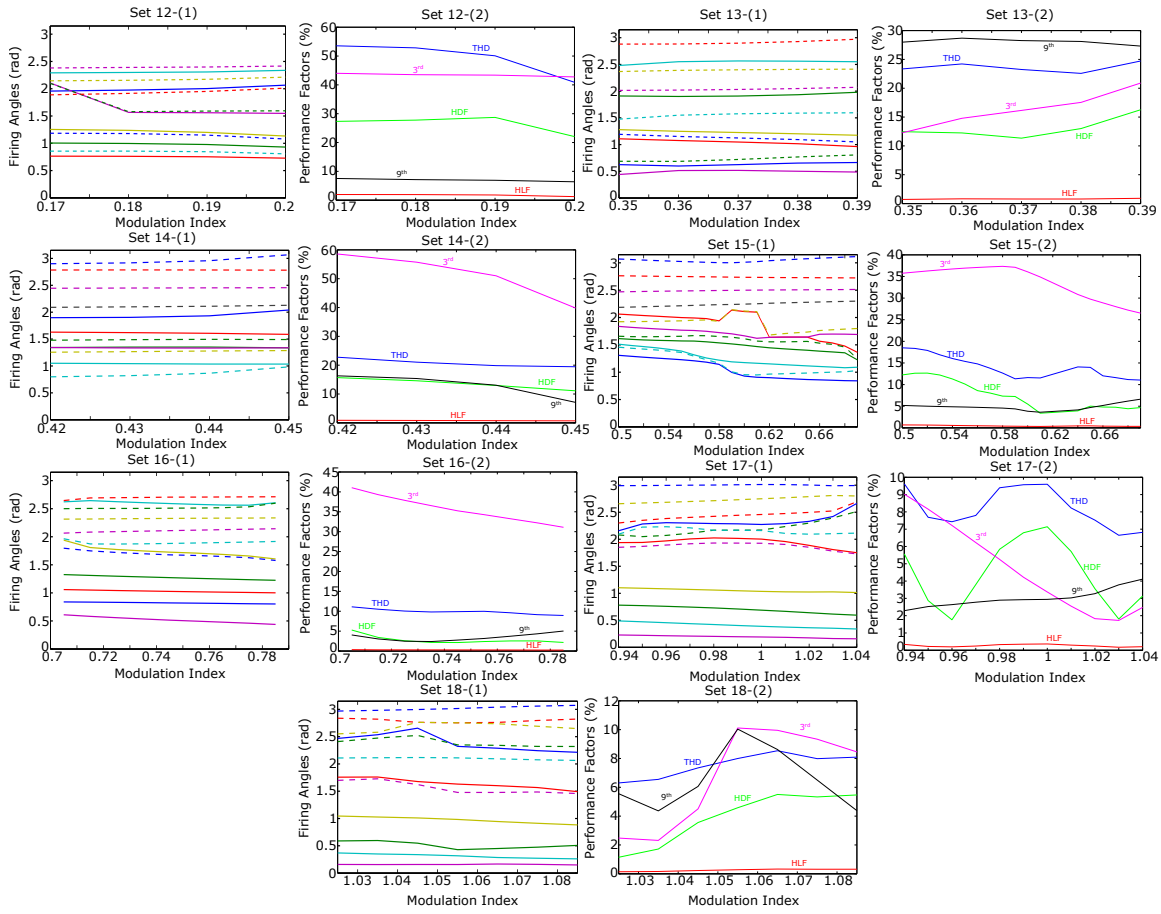Fig. 11. Continuous sets of solutions for case II-HW.

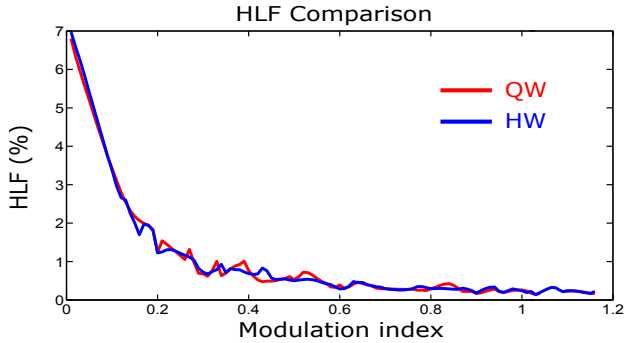Fig. 12. Continuous sets of intermediate solutions for case II-HW.

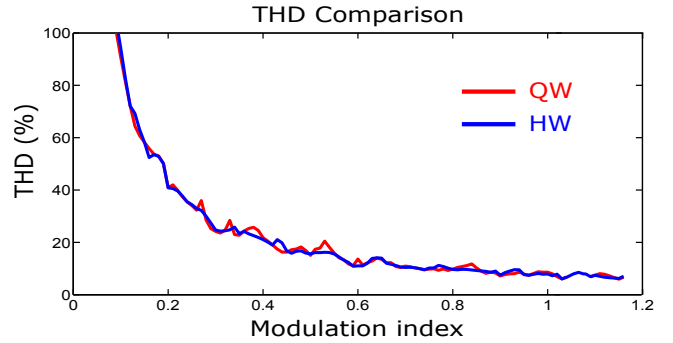Fig. 13. Harmonic loss factor (HLF) provided by QW and HW solutions (cases I-QW and II-HW).

Fig. 14. Total harmonic distortion (THD) provided by QW and HW solutions (cases I-QW and II-HW).

by different symmetries. Consequently, both symmetries should be considered to find the most suitable solution.

- Figs. 15 and 16 show the modulation index range provided by every set of firing angles obtained for cases I-QW and II-HW. As it is shown, the QW symmetry does not provide solutions for $1.04 < m_a < 1.09$. Otherwise, HW symmetry solves the problem for those m_a values. On the other hand, Figs. 15 and 16 also shows the selected set of firing angles throughout the modulation index range for QW and HW symmetries, respectively. In case of overlap of several sets of firing angles, the set which

provides the lowest HLF is selected.

All in all, it can be concluded that the increase in the number of obtained solutions, for a particular m_a, provides more options to optimize the performance factors. In this sense, the proposed universal formulation in this paper, which is able to find multiple HW solutions, increases the probability of improving the waveform design. In addition, this probability can also be increased obtaining both QW and HW solutions, instead of utilizing only one symmetry, because the number of different solutions provided for every m_a is higher.
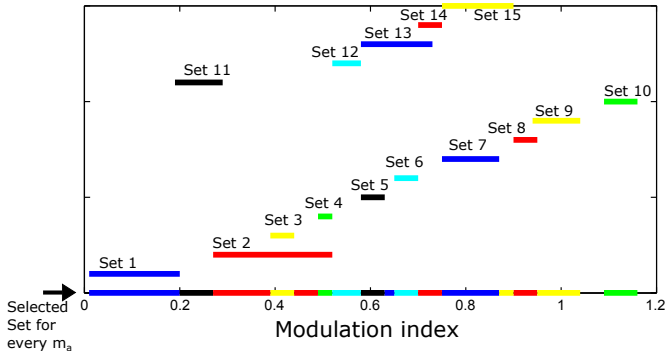
Fig. 15. Modulation index range provided by every set of firing angles of case I-QW.
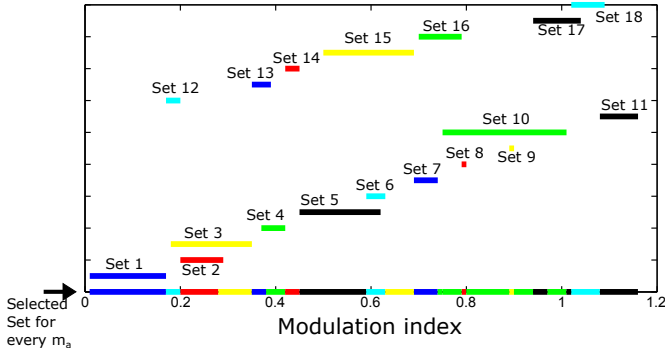

Fig. 16. Modulation index range provided by every set of firing angles of case II-HW.
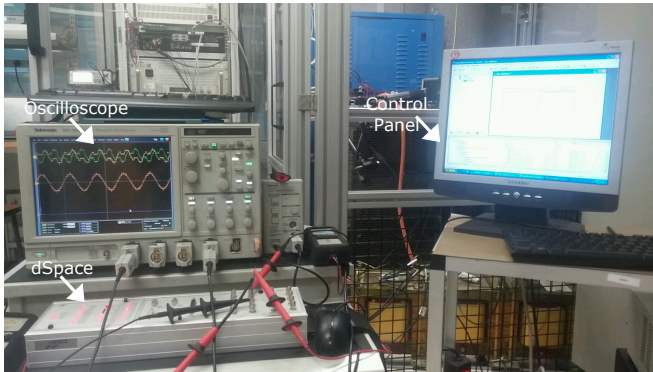

Fig. 17. Experimental set-up with dSpace 1104: control panel, dSpace and oscilloscope.

VI. EXPERIMENTAL RESULTS

The solutions provided by the proposed universal formulation with HW symmetry have been validated by experimental results obtained from a dSpace 1104. The laboratory set-up is depicted at Fig. 17. Regarding the case II-HW, SHE-PWM waveforms with HW symmetry and 9 levels have been obtained with 12 firing angles in the first HW. The experimental results have been provided using the sets of firing

angles depicted at Fig. 11. Particular samples of these sets are included in Appendix A.

The utilized sets of firing angles have been stored in look-up tables and the waveforms have been generated with the digital to analog converters (DACs), representing the gate signals of a MVSC. In this way, two different phase-neutral voltages, V_{an} and V_{bn}, have been generated, utilizing two different DACs, with the aim of obtaining both the phase-neutral voltage and the line-line voltage. Along with the experimental results, the simulation waveforms and their corresponding spectrums have also been obtained, providing the possibility of comparing both simulation and experimental results.

In particular, Figs. 18-(a) and 18-(c) show the simulation results of v_{a0} and its corresponding spectrum when $m_a = 1$. As it can be noticed, the non desired harmonics are eliminated and the first non-triplen harmonic is located in $950Hz$. On the other hand, Figs. 18-(b) and 18-(d) show the equivalent experimental results of v_{a0} and its corresponding spectrum. The harmonics are also correctly eliminated. In addition, the simulation results of line-line voltage, v_{ab} are shown in Figs. 18-(e) and 18-(g), providing the waveform and its corresponding spectrum, respectively. The spectrum shows how the first non-eliminated harmonic is located in $950Hz$ with all low order harmonics, including triplen, eliminated. Finally, Figs. 18-(f) and 18-(h) show the experimental results of V_{ab} and its spectrum. As it can be seen, the harmonics are correctly eliminated up to the 19th, which is the first non eliminated low order harmonic.

Except for small differences, an accurate correlation between simulation and experimental results can be observed, thus validating the proposed algorithm and the analysis carried out in the paper. The small differences between the simulation and experimental results are due to three reasons. First, the dSpace 1104 has computational limitations which provide an execution step of $70\mu s$. Second, the digital to analogue converter (DAC) introduces a quantization error. Finally, the oscilloscope measurements contain noise. However, these facts have a minor impact on the results.

VII. CONCLUSION

The proposed HW SHE-PWM universal formulation provides the ability to calculate simultaneously the switching patterns and the associated firing angles throughout the m_a range, without using predefined waveforms. In particular, a unique equation system which is valid for any possible waveform has been defined. On the other hand, an objective function, which can be utilized by optimization algorithms, has been designed to disregard automatically invalid solutions.

Furthermore, regarding the existing universal formulation with QW symmetry and the proposed universal formulation with HW symmetry, a process to acquire the solutions and to optimize the SHE-PWM waveform, with regard to different performance factors, has been proposed. Examples of HW and QW solutions for a converter with 9 levels have been obtained throughout the m_a range. As a result, the optimum solution, which provides the lowest HLF for every m_a, has been provided by the HW or QW symmetry, depending on
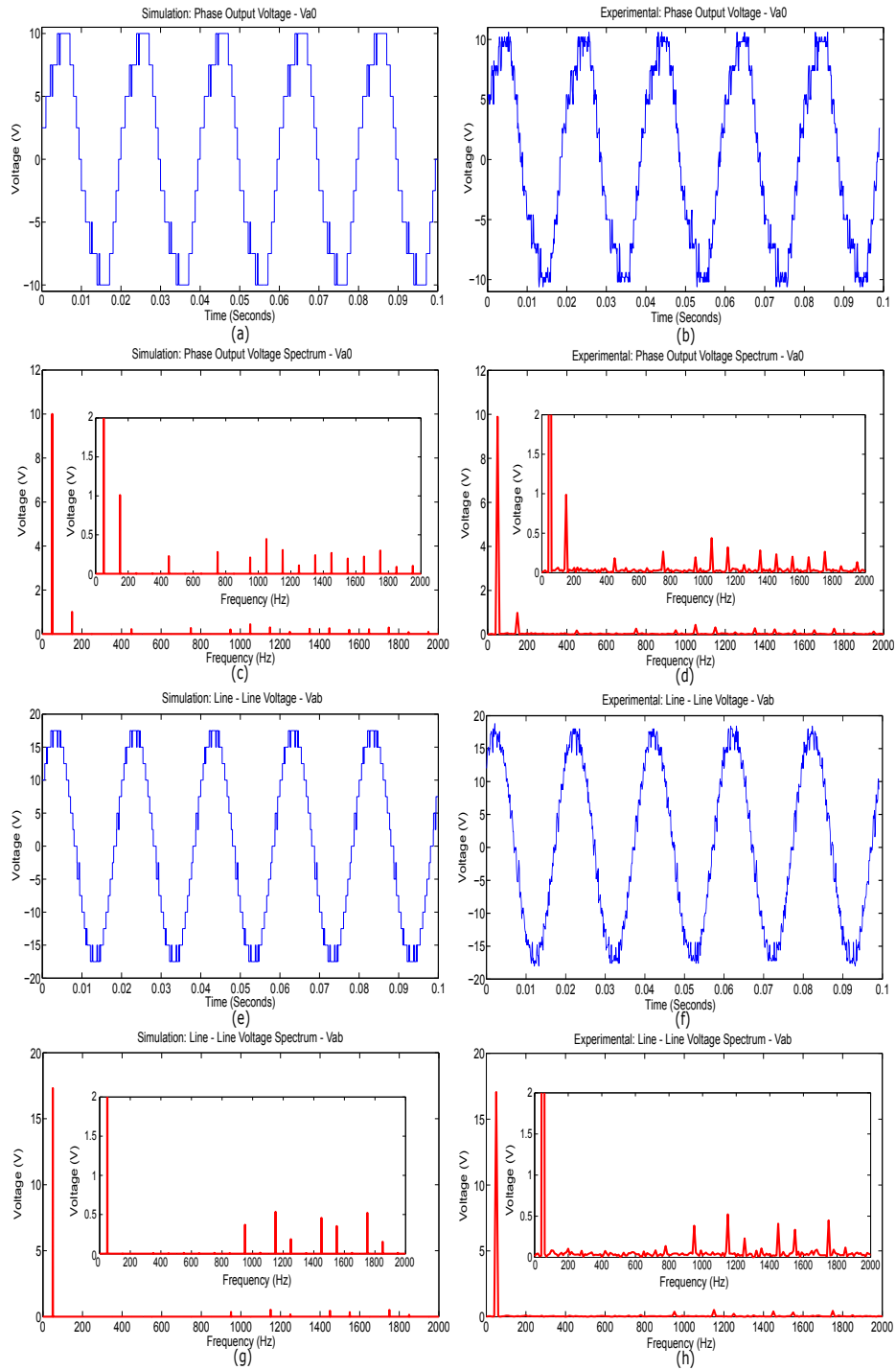
Fig. 18. Simulation and experimental results with 12 firing angles in the first HW and $f = 50$ Hz. (a) Simulation: Phase-neutral voltage (v_{an}). (b) Experimental: Phase-neutral voltage (v_{an}) (c) Simulation: Phase-neutral voltage (v_{an}) spectrum. (d) Experimental: Phase-neutral voltage (v_{an}) spectrum. (e) Simulation: Line-line voltage (v_{ab}). (f) Experimental: Line-line voltage (v_{ab}). (g) Simulation: Line-line voltage (v_{ab}) spectrum. (h) Experimental: Line-line voltage (v_{ab}) spectrum.

the m_a value. Therefore, instead of using only one symmetry, obtaining the solutions with both symmetries is recommended to optimize the design of the SHE-PWM waveform. All in all, the proposed universal formulation simplifies significantly the search process with respect to previous formulations with HW symmetry, assisting the application of SHE-PWM in multilevel converters.

APPENDIX
EXAMPLE OF SOLUTIONS PROVIDED THROUGHOUT THE
MODULATION INDEX RANGE

Table III includes the firing angles, its corresponding setp sign and the initial level of the waveform for the solutions selected in case II-HW.

TABLE III
FIRING ANGLES AND SIGN OF EVERY STEP OF HW SOLUTIONS SELECTED FOR CASE II-HW (12 FIRING ANGLES AND 9 LEVELS)

m_a	θ_1	θ_2	θ_3	θ_4	θ_5	θ_6	θ_7	θ_8	θ_9	θ_{10}	θ_{11}	θ_{12}	Initial Level
0.1	⇓0.8344	⇓1.1385	⇑1.2775	⇓1.3805	⇑1.4666	⇓1.5949	⇑1.6924	⇑1.9768	⇑2.2906	⇓2.3490	⇓2.8732	⇓3.1327	1
0.2	⇑0.0000	⇓0.2708	⇑0.7089	⇓0.7749	⇑0.9048	⇓1.1119	⇑1.3185	⇑1.5470	⇓1.5937	⇓2.0298	⇓2.2363	⇓2.4315	1
0.3	⇑0.1899	⇓0.2730	⇑0.3639	⇓0.5164	⇑0.8951	⇑1.0622	⇓1.0815	⇑1.6061	⇓1.9467	⇓2.6022	⇓2.8087	⇑2.9206	0
0.4	⇑0.4292	⇓0.7985	⇓1.1163	⇑1.1892	⇓1.5428	⇑1.6777	⇑1.9318	⇓2.4123	⇑2.4973	⇓2.7729	⇓2.9278	⇓3.1196	1
0.5	⇑0.0764	⇓0.2453	⇓1.0919	⇑1.2241	⇑1.3905	⇑1.7790	⇓1.8650	⇑2.0199	⇓2.3430	⇓2.4707	⇓2.7649	⇓3.0553	1
0.6	⇑0.1518	⇓0.5467	⇑1.1435	⇑1.1699	⇑1.4868	⇑1.6529	⇑1.9859	⇓2.0132	⇑2.4993	⇓2.6390	⇓2.7392	⇓2.9877	1
0.7	⇑0.2104	⇑0.8370	⇑1.0678	⇓1.2719	⇑1.3475	⇑1.6559	⇓1.7459	⇑1.7950	⇓1.8439	⇓2.0736	⇓2.5139	⇓2.7222	0
0.8	⇑0.3465	⇓0.3706	⇑0.4518	⇑1.2131	⇑1.8161	⇓1.8970	⇑2.0131	⇓2.1393	⇓2.3576	⇓2.7014	⇓2.8963	⇓3.0821	1
0.9	⇑0.1069	⇑0.2860	⇑0.9422	⇑1.1075	⇓1.1460	⇑1.5662	⇓1.6237	⇑1.6744	⇓2.0257	⇓2.5318	⇓2.7044	⇓2.8551	0
1	⇑0.3277	⇑0.6712	⇓0.8045	⇓0.8651	⇑1.2393	⇓1.3920	⇑1.4551	⇓2.2369	⇓2.5170	⇓2.7472	⇓2.9560	⇓3.1408	1
1.1	⇑0.0985	⇑0.2854	⇑0.4993	⇑0.8185	⇓1.9978	⇑2.1092	⇓2.2548	⇑2.3514	⇓2.3891	⇓2.6362	⇓2.8615	⇓3.1130	0

REFERENCES

[1] A. Perez-Basante, S. Ceballos, G. Konstantinou, J. Pou, J. Andreu, and I. M. de Alegria, "A universal formulation for selective harmonic elimination pwm with half-wave symmetry for multilevel voltage source converters," in *Proc. of Annual Conference of the IEEE Industrial Electronics Society (IECON)*, Oct 2016, pp. 3207 – 3212.

[2] J. Huber and A. Korn, "Optimized pulse pattern modulation for modular multilevel converter high-speed drive," in *Proc. of Power Electronics and Motion Control Conference (EPE/PEMC)*, Sept 2012, pp. LS1a–1.4–1 – LS1a–1.4–7.

[3] R. P. Aguilera, P. Acua, P. Lezana, G. Konstantinou, B. Wu, S. Bernet, and V. G. Agelidis, "Selective harmonic elimination model predictive control for multilevel power converters," *IEEE Transactions on Power Electronics*, vol. 32, no. 3, pp. 2416–2426, March 2017.

[4] S. Rohner, S. Bernet, M. Hiller, and R. Sommer, "Modulation, losses, and semiconductor requirements of modular multilevel converters," *IEEE Transactions on Industrial Electronics*, vol. 57, no. 8, pp. 2633 – 2642, Aug 2010.

[5] J. Rodriguez, S. Bernet, B. Wu, J. Pontt, and S. Kouro, "Multilevel voltage-source-converter topologies for industrial medium-voltage drives," *IEEE Transactions on Industrial Electronics*, vol. 54, no. 6, pp. 2930 – 2945, Dec 2007.

[6] M. Dahidah, G. Konstantinou, and V. Agelidis, "A review of multilevel selective harmonic elimination pwm: Formulations, solving algorithms, implementation and applications," *IEEE Transactions on Power Electronics*, vol. 30, no. 8, pp. 4091 – 4106, Aug 2015.

[7] G. Konstantinou, M. Ciobotaru, and V. Agelidis, "Selective harmonic elimination pulse-width modulation of modular multilevel converters," *IET Power Electronics*, vol. 6, no. 1, pp. 96 – 107, Jan 2013.

[8] M. S. A. Dahidah and V. Agelidis, "Selective harmonic elimination pwm control for cascaded multilevel voltage source converters: A generalized formula," *IEEE Transactions on Power Electronics*, vol. 23, no. 4, pp. 1620 – 1630, July 2008.

[9] M. Dahidah, G. Konstantinou, N. Flourentzou, and V. Agelidis, "On comparing the symmetrical and non-symmetrical selective harmonic elimination pulse-width modulation technique for two-level three-phase voltage source converters," *Power Electronics, IET*, vol. 3, no. 6, pp. 829 – 842, Nov 2010.

[10] T. Liang, R. O'Connell, and R. Hoft, "Inverter harmonic reduction using walsh function harmonic elimination method," *IEEE Transactions on Power Electronics*, vol. 12, no. 6, pp. 971 – 982, Nov 1997.

[11] J. Chiasson, L. Tolbert, K. McKenzie, and Z. Du, "A new approach to solving the harmonic elimination equations for a multilevel converter," in *Proc. of Industry Applications Conference (38th IAS Annual Meeting)*, vol. 1, Oct 2003, pp. 640 – 647.

[12] J. N. Chiasson, L. M. Tolbert, Z. Du, and K. J. McKenzie, "The use of power sums to solve the harmonic elimination equations for multilevel converters," *European Power Electronics and Drives Journal*, vol. 15, no. 1, pp. 19 – 27, February 2005.

[13] F. Filho, H. Maia, T. Mateus, B. Ozpineci, L. Tolbert, and J. Pinto, "Adaptive selective harmonic minimization based on anns for cascade multilevel inverters with varying dc sources," *IEEE Transactions on Industrial Electronics*, vol. 60, no. 5, pp. 1955 – 1962, May 2013.

[14] A. I. Maswood, S. Wei, and M. Rahman, "A flexible way to generate pwm-she switching patterns using genetic algorithm," in *Proc. of Applied Power Electronics Conference and Exposition (APEC)*, vol. 2, 2001, pp. 1130 – 1134.

[15] K. El-Naggar and T. Abdelhamid, "Selective harmonic elimination of new family of multilevel inverters using genetic algorithms," *Energy Conversion and Management*, vol. 49, no. 1, pp. 89 – 95, 2008.

[16] Z. Salam, A. Majed, and A. Amjad, "Design and implementation of 15-level cascaded multi-level voltage source inverter with harmonics elimination pulse-width modulation using differential evolution method," *IET Power Electronics*, vol. 8, no. 9, pp. 1740 – 1748, 2015.

[17] H. Taghizadeh and M. Hagh, "Harmonic elimination of cascade multilevel inverters with nonequal dc sources using particle swarm optimization," *IEEE Transactions on Industrial Electronics*, vol. 57, no. 11, pp. 3678 – 3684, Nov 2010.

[18] D. Ahmadi, K. Zou, C. Li, Y. Huang, and J. Wang, "A universal selective harmonic elimination method for high-power inverters," *IEEE Transactions on Power Electronics*, vol. 26, no. 10, pp. 2743 – 2752, Oct 2011.

[19] H. Huang, S. Hu, and D. Czarkowski, "A novel simplex homotopic fixed-point algorithm for computation of optimal pwm patterns," in *Proc. of Power Electronics Specialists Conference (PESC)*, vol. 2, June 2004, pp. 1263 – 1267.

[20] S. G. Rosu, C. Radoi, A. Florescu, P. Guglielmi, and M. Pastorelli, "The analysis of the solutions for harmonic elimination pwm bipolar waveform with a specialized differential evolution algorithm," in *Proc. of International Conference on Optimization of Electrical and Electronic Equipment (OPTIM)*, May 2012, pp. 814 – 821.

[21] A. Perez-Basante, S. Ceballos, J. Pou, M. Liserre, G. Konstantinou, and I. M. de Alegria, "Circulating current control for modular multilevel converter based on selective harmonic elimination with ultra-low switching frequency," in *Proc. of European Conference on Power Electronics and Applications (EPE-ECCE)*, Sept 2016.

[22] A. Perez-Basante, S. Ceballos, G. Konstantinou, J. Pou, J. Andreu, and I. M. de Alegria, "(2n+1) selective harmonic elimination-pwm for modular multilevel converters: A generalized formulation and a circulating current control method," *IEEE Transactions on Power Electronics*, vol. PP, no. 99, pp. 1 – 1, 2017.

[23] K. Yang, Q. Zhang, J. Zhang, R. Yuan, Q. Guan, W. Yu, and J. Wang, "Unified selective harmonic elimination for multilevel converters," *IEEE Transactions on Power Electronics*, vol. 32, no. 2, pp. 1579 – 1590, Feb 2017.

[24] K. Yang, Q. Zhang, R. Yuan, W. Yu, J. Yuan, and J. Wang, "Selective harmonic elimination with groebner bases and symmetric polynomials," *IEEE Transactions on Power Electronics*, vol. 31, no. 4, pp. 2742 – 2752, April 2016.

[25] G. Konstantinou and V. Agelidis, "On re-examining symmetry of two-level selective harmonic elimination pwm: Novel formulations, solutions and performance evaluation," *Electric Power Systems Research*, vol. 108, pp. 185 – 197, 2014, "".

[26] W. Fei, X. Du, and B. Wu, "A generalized half-wave symmetry she-pwm formulation for multilevel voltage inverters," *IEEE Transactions on Industrial Electronics*, vol. 57, no. 9, pp. 3030 – 3038, Sept 2010.

[27] B. Ozpineci, L. M. Tolbert, and J. N. Chiasson, "Harmonic optimization of multilevel converters using genetic algorithms," *IEEE Power Electronics Letters*, vol. 3, no. 3, pp. 92 – 95, Sept 2005.

[28] M. S. A. Dahidah and V. G. Agelidis, "A hybrid genetic algorithm for selective harmonic elimination control of a multilevel inverter with non-equal dc sources," in *Proc. of International Conference on Power Electronics and Drives Systems ((PEDS))*, vol. 2, 2005, pp. 1205 – 1210.

[29] M. S. Dahidah and V. G. Agelidis, "Generalized formulation of multilevel selective harmonic elimination pwm: Case i -non-equal dc sources,"

in *Proc. of IEEE Power Electronics Specialists Conference (PESC)*, June 2006, pp. 1 – 6.

[30] M. S. A. Dahidah and M. V. C. Rao, "A hybrid genetic algorithm for selective harmonic elimination pwm ac/ac converter control," *Electrical Engineering*, vol. 89, no. 4, pp. 285 – 291, 2007.

[31] V. G. Agelidis, A. Balouktsis, and I. Balouktsis, "On applying a minimization technique to the harmonic elimination pwm control: the bipolar waveform," *IEEE Power Electronics Letters*, vol. 2, no. 2, pp. 41 – 44, June 2004.

[32] V. G. Agelidis, A. Balouktsis, I. Balouktsis, and C. Cossar, "Multiple sets of solutions for harmonic elimination pwm bipolar waveforms: analysis and experimental verification," *IEEE Transactions on Power Electronics*, vol. 21, no. 2, pp. 415 – 421, March 2006.

[33] G. S. Konstantinou and V. G. Agelidis, "Bipolar switching waveform: Novel solution sets to the selective harmonic elimination problem," in *Proc. of IEEE International Conference on Industrial Technology (ICIT)*, March 2010, pp. 696 – 701.

[34] Z. Michalewicz, *Genetic algorithms + Data structures = Evolution programs*. Springer Science & Business Media, 1996.

[35] V. G. Agelidis, A. I. Balouktsis, and C. Cossar, "On attaining the multiple solutions of selective harmonic elimination pwm three-level waveforms through function minimization," *IEEE Transactions on Industrial Electronics*, vol. 55, no. 3, pp. 996 – 1004, March 2008.

[36] G. Konstantinou, "Harmonic elimination pulse width modulation of modular and hybrid multilevel converter topologies," Ph.D. dissertation, The University of New South Wales (UNSW), 2012.

[37] J. Kumar, B. Das, and P. Agarwal, "Selective harmonic elimination technique for a multilevel inverter," in *Proc. of Fifteenth National Power Systems Conference (NPSC)*, Bombay, India, 2008.

[38] W. Fei, X. Ruan, and B. Wu, "A generalized formulation of quarter-wave symmetry she-pwm problems for multilevel inverters," *IEEE Transactions on Power Electronics*, vol. 24, no. 7, pp. 1758 – 1766, July 2009.

[39] M. Balasubramonian and V. Rajamani, "Design and real-time implementation of shepwm in single-phase inverter using generalized hopfield neural network," *IEEE Transactions on Industrial Electronics*, vol. 61, no. 11, pp. 6327 – 6336, Nov 2014.

[40] W. Fei, B. Wu, and Y. Huang, "Half-wave symmetry selective harmonic elimination method for multilevel voltage source inverters," *IET Power Electronics*, vol. 4, no. 3, pp. 342 – 351, March 2011.

[41] A. Sanchez-Ruiz, G. Abad, I. Echeverria, I. Torre, and I. Atutxa, "Continuous phase-shifted selective harmonic elimination and dc-link voltage balance solution for h-bridge multilevel configurations, applied to 5l hnpc," *IEEE Transactions on Power Electronics*, vol. 32, no. 4, pp. 2533–2545, April 2017.